CHAPTER IV

Implementation

As a most active research issue in the contexts of manipulator control, adaptive control has not yet achieved great success as one of the most promising control strategy. This is due to the fact that a few of expermental results obtained from actual hardware implementation on existing robot manipulators can demonstrate significant improvement in performance over the conventional fixed gain controllers. This is also true for that most of available commercial robotic systems are still acceptably performing its tasks by utilization of the fixed gain control scheme. In a past few year, considerable paper in adaptive control of robot manipulators have been contineuously proposed. Many control algorithms were synthesized and tested mostly by computer simulation based on the mathematical model of a manipulator. A very few of experimental results implemented on actual systems have been reported. The study and evaluation of the adaptive control scheme by theoretical analysis and computer simulation are, although, nescessary as efficient tools for investigating the problems but for very complex dynamic systems, such as robot manipulators, they are not sufficient. Essential nonlinearities inhered in dynamic system of manipulators prevent us from direct analysis by the throughly-discovered linear system theory and the results from simulation can not exactly represent dynamics of the real system. There is, however, nonlinear system theory that can be directly used to analyze nonlinear systems. Basic principles of Lyapunov methodology that had founded analitical footing of the nonlinear system theory are not restricted only for linear systems. Nevertheless, in the case of manipulator dynamics, it is still very difficult for direct mathematical analysis due to its huge structure and the strong nonlinearity of the dynamic equations even when simple configuration of a manipulator is discussed.

For adaptive manipulator control which is a unique class of nonlinear, time-varying, multiinput-multioutput dynamic systems and has its own specific dynamic features, experimental evaluation would be, in addition to computor simulation, the ultimate way of justification for the applicability of the control scheme. Since it is a common truth that like the dynamic model can never be matched with the real physical system we, also, can never account for all existing signals generated within the real robot manipulator during operation and, of importance, some of them usually neglected in stability analysis. This may lead the system close to maginally-stable region or even to be unstable when inherent factors that are unmodeled, measurement noise and high-frequency dynamics neglected are randomly stimulated to have significant magnitude during performing. Based on this point of view, we shall establish experimental evaluation on the proposed self-tuning scheme with the Chula2 manipulator performing path tracking. To be comparable in the issues of stability robustness and tracking performance, we shall implement and experiment the PD control scheme as a conventional fixed-gain controller, that has been prooved to be successful in commercial robotic systems even in trajectory tracking tasks and has its strength on robustness and stability over some proposed adaptive schemes.

4.1 The Chula2 Robot Manipulator

4.1.1 Introduction

The Chula2 robot manipulator is the second robot manipulator designed and constructed at the Control System Laboratory, Chulalongkorn University for educational purpose. It is used as a basic controlled plant for general control algorithm implementation. The main goal in the design of our first manipulator, the Chula1, is to construct a simply configurated mechanism with its control hardware composed of low cost and affordable components such as a PC compatible microcomputer and its peripheral interface cards. As the needs in industrial applications directed into more precisely manipulation task that requires more and more sophisticated robot operating with higher precision in

trajectory tracking manner. The Chula2 project was created in 1988. With capabilities to do industrial manipulation tasks such as a most common in product assembly line in factory, pick-and-place job, the manipulator design also still maintains the concept of using low cost microcomputer and its advanced accessories as control hardware in mind. After we had considered servoing performance and noticed some problems occurred with the Chula1, we had decided to design a new manipulator that has different mechanism configuration to suit for some types of task manipulation. In order to improve performance and acquire high accuracy of tracking motion, control hardware of the Chula2 had been carefully designed using digital techniques. For the issue of computational power, the new controller utilizes two PC/AT compatible microcomputer working in parallel. This computing facility can afford satisfactory computing power for simultaneous servoing and parametric estimation. The controller, as a whole, permits the manipulator to execute path tracking at rather high speed in real-time fashion.

4.1.2 Summary of the Chula1 Robot Manipulator

The Chula1 robot manipulator was constructed in 1986 and capable of only point-to-point joint motion. We merely wanted to use it as a laboratory tool for introductory DC motor control course. The arm of the Chula1 was made from aluminium for minimum weight and configured to be articulated manipulator type with three rotary joints. Its joints are actuated by DC servo motors with 1:100 gears excluding the third joint composition that is additionally equipped with 1:1 belt drive extending from gear output to joint shaft allowing the motor to be installed at lower position so that the gravitational effect on the motor body can be kept minimum. The position feedback comes from linear potentiometers installed at the output shaft end of the joints. The Chula1 configuration is shown in Figure 4.1

The controller comprises a PC/XT compatible microcomputer and a 12-bit A/D, D/A interface card used as computing portion and data acquisition portion to complete servo loop. The

control algorithm implemented was three simple independent PID loops of DC motors for each of three joints. The resultant system was fairly in performance for point-to-point movement but its static accuracy was rather poor due to limitation on qualities of our equipments used.

As we use this simple manipulator as a vehicle to survey some important problems that will arise in controlling a DC- motor-actuated manipulator, we can summarize the main problems discovered from the Chula1 manipulator into many points in the followings

1. With a PC/XT compatible microcomputer as servo computing facility, the low cost simple point-to-point control purpose is fairly satisfied. But in order to advance into exploitation of more sophisticated control for high performance tracking purpose, making use of one microcomputer to construct a manipulator's controller is currently far from being feasible.

2. Position feedback by potentiometers, although has linear characteristic, subjects to many sources of noise, first from its power supply, second from noise generated within itself as common resistive noise and electromagnetic-induced high frequency noise content that can be caused along the transmission lines from the manipulator and potentiometer body, electrical signal wires, connecters to interconnection with A/D converter. Hence accuracy of position measurement is degraded.

3. The use of aluminium material to built the arm body makes mechanical structure much flexible. This causes less structure stiffness that tends to induce low-frequency mechanical resonance during actuating the arm.

4. Due to the use of linear DC servo motor in velocity servo loop, we must operate the motor at high speed so that power generated by the motor will be high enough to drive the arm against gravity and achieve desire position, but joint operating velocity is very low relative to motor speed. This fact directs to making use of speed reducer such common and inexpensive as a gear box. Every gear always presents some backlash that introduces strong nonlinearity into the dynamics and can decreases position accuracy.

4.1.3 Design Specifications of the Chula2 Robot Manipulator

The design phase of the Chula2 project was started in the early of 1988. We had the objective of building a high performance robot manipulator that is capable of trajectory tracking. Based on information of control problems from the Chula1 manipulator, we had set performance requirements and design specifications for directing the research to meet the goals. They came as follows.

A. Geometric Configuration

The principal purpose of the Chula2 configuration design is to simplify mathematical terms in the kinematic equations and also, consequently, the structure of the dynamic equations. With the goal to design a robot manipulator that can be easily adapted further for industrial applications it must be configured to suit for some human-like manipulation tasks. We used a conventional task of general product assembly line in factory, pick-and-place job, as a case and with the need of high performance in continuous path tracking motion, we recognized path tracking capability of the Chula2 in the design. Account for these two purposes and append with the sake of simplicity in detail constructing and assembling including maintenance, we had decided to choose SCARA configuration for the Chula2. The manipulator will have work envelope of cylindrical shape with 0.50-meter vertical travel and 0.70-meter cylindrical radius. The whole design of the robot will have six self-actuated joints to obtain six degree-of-freedom manipulation. Common with other SCARA manipulators planar reach occurs from actuating of the first two vertical rotary joints and vertical distance can be obtained by translation of the third joint. The three-axis wrist will be attached at the end of the third link for 3-dimension orientation. The wrist construction will be in the later phase.

B. Accuracy and Speed

Accuracy during trajectory tracking is of most interest in our case as it is one of our major research issue. Speed requirement for the Chula2 is not critical. We specified desired tracking accuracy at moderate speed. It is, however, our target that the average tracking speed in planar reach should not be less than 0.5 m/s and the maximum vertical travel speed of 0.8 m/s should be achieved. In order to achieve high servo accuracy, we will make use of digital techniques in every steps along sensors to data acquisition system in the system controller. Incremental optical encoders will be used for position and speed sensing. They will be installed at each motor shaft end before speed reducer attachment. This composition augmented with very high resolution of the optical encoders used will permit very high resolution of joint coordinate sensing. With the use of a 1: 160 harmonic gear as a speed reducer or torque amplifier, the resolution of each joint coordinate should not be more than 10 microradians for rotary joints and at least, 10 microns resolution should be achieved for translational joint comprising motor and ball screw composition working as rotary-to-linear motion converter. The effective tracking accuracy in three dimensions that we prefer should be within 0.5 mm, although we have got typical encoder accuracy of only +/- 1 LSB. Additional mechanical error we expect will come from small mechanical tolerance, clearance and backlash unavoiding in mechanism installation including flexibility of the material used.

C. Payload

We had considered an optimum case when the gripper and equipped sensors are carrying a payload of 5 kg. at maximum design speed. With this requirement, we can specify a maximum amount of actuating torque needed from actuators at each joints. Size and model of the actuators can then be selected to properly match with the requirement. The use of aluminum alloy that we preferred will then be justified for its static and dynamic loading capability. Stiffness of the arm body is another issue that is of importance in dynamic response considerations. We will make use of

this property estimated from strength data of material and specification of payload to investigate for mechanical resonance and other vibrational characteristics of the manipulator mechanism.

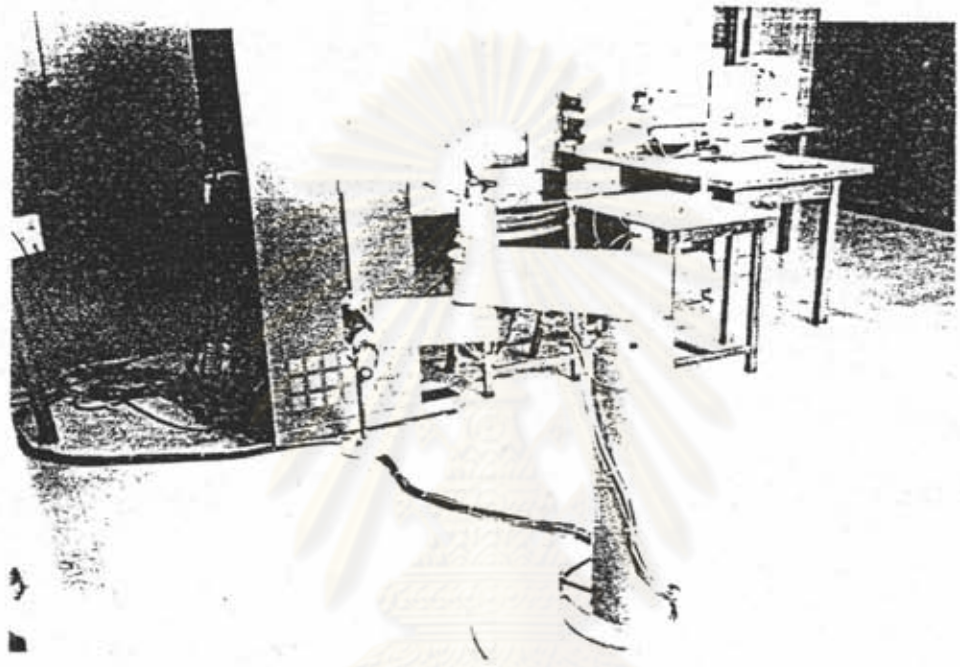

Figure 4.1: The Chula2 manipulator

4.1.4 Mechanical System Designs

According to our research direction, we decided to divide the whole Chula2 project into two phases of design and construction of mechanical system corresponding to two basic effective movement of manipulators, translation and orientation of its end effector. The first three joints of the Chula2 manipulator are applied as the least configuration for doing translation of the end effector in three dimensions. Whereas the end effector orientation can be obtained from operation of a three-axis

wrist which is to be constructed in the second phase, attached next to end of the third link of the arm. At the time of this presentation, we had completed the first phase of the project as the three-axis arm was already designed and constructed. Its final configuration is shown in Figure 4.1.

A. Manipulator Arm

The configuration as shown allows the arm to cover 1.5 m^2 of horizontal circular area caused from 0.7 m maximum radius reach. The range of joint 1 rotation was limited to be 270 degrees. Restricted by the geometrics of link 3, we permit joint 2 to be rotate within range of 180 degrees. Two couple of infrared sensors were installed to detect limits of angle. Joint 3 has vertical travel range of 0.5 m. yielded from prismatic mechanism comprising DC motor, shaft coupling and ball screw package. The total work volume is turned out to be about 0.5 m^3 of cylindrical wall shape. It is suitable for pick-and-place job purpose as we previously specified.

Structural design of the arm was done following the concept of having maximum structural stiffness as much as possible while yielding minimum weight mechanism that is conventional requirement in general manipulator design. For detailed mechanical design of machined parts, we took into account the sake of simplicity in machining, assembly and installation in addition to mechanical precision. The number of machined parts was kept minimum and high precision machine tools were used to elaborate these parts. Light-weight Aluminum alloy was used to make most of parts of the arm body. Although increasing weight, some of structural parts, such as joint shafts and associated coupling with motor shafts, were made by stainless steel to gain joint strength and stiffness. High quality bearings were used to support joint rotation relative to motors and arm body with less friction. In order to free joint composition of the first two joints which have joint axes of vertical orientation from gravitational force, low-friction trust bearings were installed to transfer whole weight of joint composition to joint aluminum housing. All of these parts had been accurately machined for mechanical precision when they were totally assembled. The base of the arm was

design to support whole weight of the arm and have its own weight as much as possible to increase total inertia of the whole arm for the purpose of having good vibrational behavior. It was constructed from conventional steel pipe of 80 kg. weight. And it allows the motor-gear housing of the first joint to be installed inside.

B. Joint Composition

As we emphasize to effectively making use of harmonic gears to obtain zero backlash speed reduction, the composition was to be carefully designed and high precision machining of every parts involved was needed. Each of three joints has its unique composition due to different motors and gears used.

Joint 1

The aluminum alloy housing of the joint was installed inside the base steel pipe for the sake of compactness. An Electro-craft moving-magnet DC servo motor was used as a joint actuator. Harmonic drive model which can withstand maximum torque of 9000 Nm. was equipped with the motor shaft. Its outer teethed ring and the motor casing were fixed with aluminum alloy housing. The output cylinder of the harmonic drive was rigidly coupled to the body of the second link. We inserted a trust bearing to support the weight of link 2 while offering very low friction relative rotation between touching surfaces of link 1 and link 2. The bearing cooperated with a ball bearing between joint shaft and aluminum housing can, instead of joint shaft, withstand bending moment occurred by weight of further arm span leaving the joint shaft for delivering actuating torque alone. For position and velocity feedback, an incremental optical shaft encoder of the Suntax model with a resolution of 2048 pules per one shaft revolution was asserted at another side of the motor shaft. We did not use tachometer signal, although was embodied with the motor housing from factory, as a velocity feedback signal in servo loop for that we can digitally extract velocity content from

measurement of encoder pulse frequency instead. This joint configuration can offer a resolution of more than 1,300,000 steps per one revolution of the joint shaft corresponding to a step size of less than 5 microradians.

Joint 2

It is one of our objectives to utilize the manipulator as a general control apparatus, we intended to select various equipments to build its mechanism. We had selected a moving-coil DC motor as an actuator of joint 2. The motor has very low rotor inertia allowing the joint to be more dexterous. Although it has rather low torque exerting capability relative to the moving-magnet motor, when cooperating with the harmonic drive possessing high value of speed reduction ratio, the composition can excessively exert driving torque for operating condition of joint 2 which has much lower link inertia than the previous joint according to the configuration. The joint subjects to a few microradians of backlash due to the use of a flat-type 1:160 harmonic drive for the sake of joint compactness. The composition of a moving-coil motor and a flat-type harmonic drive that possesses much lower rotational inertia than joint 1 can deliver much more acceleration with higher maximum speed. For position sensor, a Renco incremental optical shaft encoder with a moderate resolution of 1000 pulses per revolution was installed at the front of the motor shaft before the shaft coupling with the harmonic gear. The resultant joint resolution is 1.024 microradians excessively high for very accurate position measurement.

Joint 3

This joint is prismatic for doing vertical translation. We used the nearly zero-backlash composition of worm gear and ball screw to convert rotary motion into translational motion perpendicular to the rotation axis. A high power and compact-size model of An Electro-craft moving-magnet DC servo motor which can deliver maximum power of 500 watts was directly

coupled to the shaft of the worm gear. Since the worm gear and ball screw composition has rather low rotational friction. It, therefore, possesses high mechanical efficiency of power transmission. This power transmission system is quite satisfactory and can carry a payload of more than 5 kg. with 0.3 m/s vertically travel speed. This performance matches with the proposed payload and speed requirements. The same type and model of a Suntax optical encoder as in joint 1 was used yelling a position resolution of less than 0.1 microns.

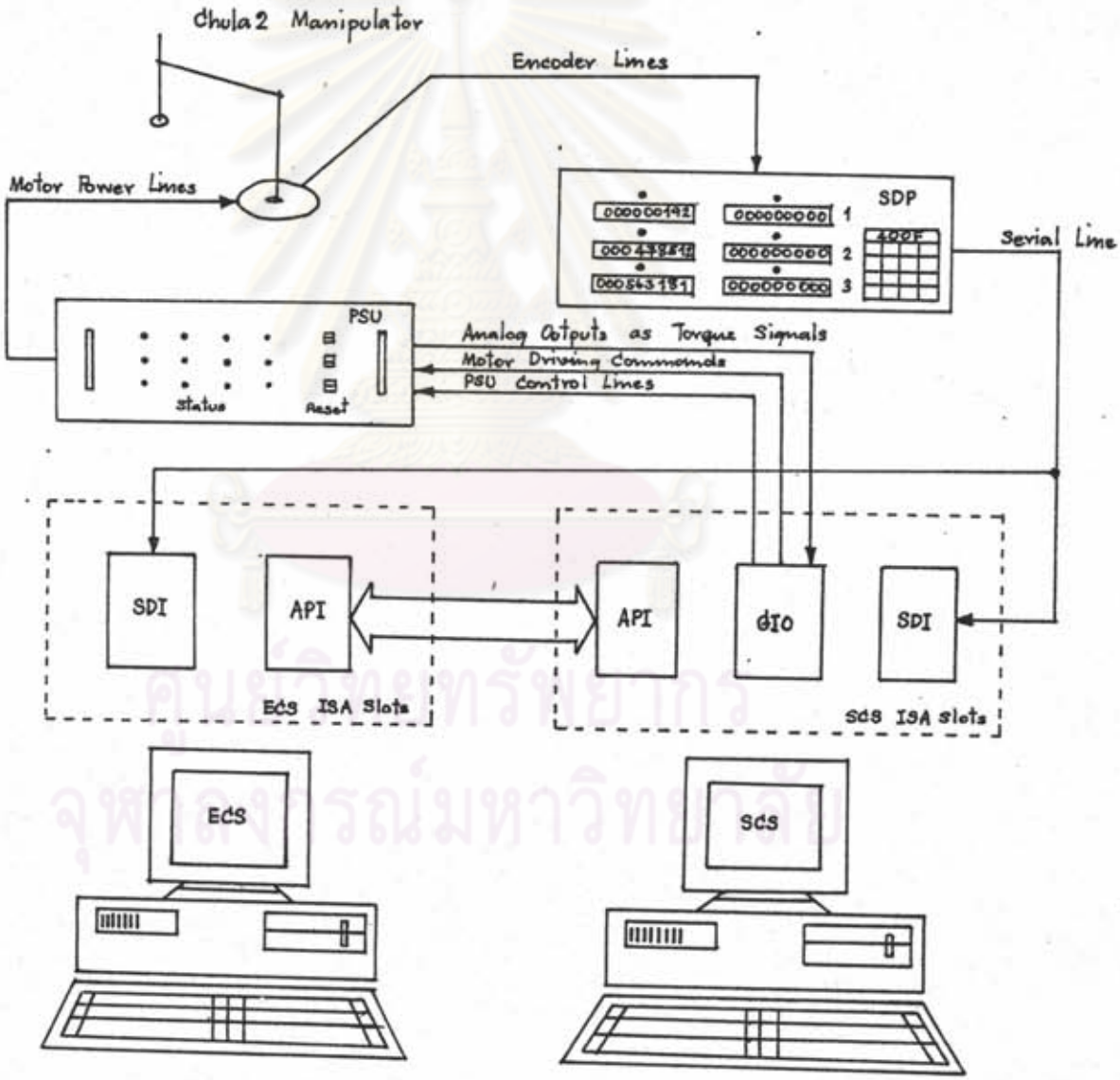

Figure 4.2: System interconnection of the Chula2 control hardware

4.1.5 Control Hardware Designs

A. Microcomputer Controllers

The Chula2 manipulator is designed for high performance tracking purpose. It sometime operates at rather high speed. The controller used with it must be able to provide sufficient sampling rate over all the operating range to validly track instantaneous kinematical information. As we aforementioned that one of the goals of the Chula2 project is to provide a basic apparatus, as a highly nonlinear controlled plant, for investigating nonlinear control problems and implementing advanced control schemes such as adaptive control or modern non-adaptive robust control, the controller we had to design must be very flexible architecture for simplicity of various scheme implementation and applications. With these requirements, the concept of using a low cost microcomputer as system controller is difficult to be possible because of limitation of its computing power. We have discussed the issue with relative to recent experimental papers that implementation of most of advanced adaptive control schemes requires minicomputer-level of computational power to achieve sufficient sampling frequency.

In discussion of computational requirement, we referred to the proposed self-tuning scheme as extreme computational burden. The composition of the control hardware must be capable of real-time processing and controlling. We expected an Intel 80386-based PC/AT compatible microcomputer which at that time possesses the fastest processing speed among microcomputers. Yet it can not offer fast enough servo rate due to huge mathematical terms in the algorithm to be computed in a real-time fashion. In spite of facing with computing speed problem, however, we had still agreed that an advantage of using a microcomputer lies in its open bus architecture which is industry standard. The microcomputer, usually referred as the PC, permits external electronic hardware to communicate with it or even with other microcomputer in the easy way. Furthermore, the way of communicating or cooperating can be customized to extremely match with our rigorous

requirements. Inspired by this fact, we turned our attention to exploitation of more than one PC working in parallel as the Chula2 system controller.

To effectively utilize this controller structure, we have to properly break down all work in general control schemes into many specific jobs relevant to its applications and real hardware implementation. After we had considered basic work done by all parts of general controllers, we can summarize and then generally determined that a microcomputer, as a computing facility in a control system, may be considered to perform two basic jobs. The first is to do computing jobs that do not involve with any hardware operation. For an overview of control schemes, this part is usually incorporated as minor loops enhancing servo capabilities of the main feedback loop which contains all necessary control equipments including real controlled plant. In the case of adaptive control, an adaptation part of the scheme is an instance. The part have to be done to offer more correct parameter information to the other part of the scheme. All of its work will be done within one section of computer program operationally irrelevant to any control equipments. The second aspect of the control computer is to be utilized as an control equipment together with actuators, sensors, controlled plant and additional control hardware to complete the principal feedback servo loop of the whole control system.

Based on these concepts, two PC compatible microcomputers are used to perform the two basic jobs as described above. The one acts as Enhanced Computing Station (ECS) for computing augmented algorithms upon control scheme implemented. Another one is to perform the feedback servo. We name it, correspondingly to the first one, Servo Computing Station (SCS) reflecting its task to be performed. For system interconnections, we decided to custom-design and build all necessary interfaces to obtain optimal system performance. Data transmission between the two microcomputers had been considered to be critical subsystem for overall data throughput. We preferred direct and fastest way to transmit computed information between them. Data transfer must be bidirectional and asynchronous in timing for retaining flexibility of various scheme implementation. A simple but fast asynchronous parallel communication interface had been

specifically devised using low cost Intel CPU peripheral VLSI chips. The interface can offer parallel communication with little CPU attention through fast hardware interrupt mechanism. Data to be transferred such as parameter estimates computed by one computer will be transformed into a sequence of characters and directly outputed to another computer upon interrupt request. By this means, data throughput will be satisfactory fast yelling functional independence of the two microcomputers . The two microcomputers can independently execute its own computing job at the same time that correspondence between them are continuously and inherently taking place. Furthermore, the functional characteristics of the correspondence can be easily reconfigured by software to optimally suit for the control algorithm to be applied.

An IBM PC/AT compatible microcomputer with 16 MHz-80286 Central Processing Unit (CPU) augmented with 80287 math-coprocessor was selected to working as the SCS. It is equipped with all dedicated custom-designed peripheral interfaces composing data acquisition unit and Digital-to-Analog converter as output unit to signal torque command into servo amplifiers. Accompanied with servo amplifiers, Motor, manipulator mechanism and sensors, the computer will represent the rest of all necessary control equipments to sufficiently complete the basic feedback servo loop. The conventional fixed-gain controller can then be applied by utilization of this adequate configuration. To enhance the main feedback loop with algorithm-oriented minor loops upon an advanced control scheme implemented which usually possesses a large amount of computational burden, we had selected the fastest 25 MHz-80386 PC/AT microcomputer for this task. The microcomputer, with floating point enhancement by 80387 math-coprocessor can deliver nearly-minicomputer computing speed up to 4 mips (million instructions per second) adequate for heavily computing tasks such as those in the self-tuning scheme that we will experiment on the Chula2.

In cooperation, the SCS will serially receives encoder information form the Servo Data Processor (SDP). The serial information will be transformed into 16-bit word and the Direct-Memory-Access (DMA) function will be invoked without CPU attention to acquire the data word

into the computer's memory. At the same instant, the same operation will also take place in the ECS. Overall data throughput of the operation is maximum at 500 Hz for three-joints manipulation. As a result, the two computer can simultaneously realize kinematic situation every 2 msec. Depend on the control scheme used, the main control program in the SCS will command the action and control timing of the correspondence facility. As a worse case of communication burden and further violating by maximum speed of DMA transfer of encoder information, processing capability of the two computer will be decreased about 8-10%. Yet, satisfactory computing performance is retained.

B. Data Acquisition and Output Unit

The resolution and accuracy of this unit is of the most important for obtaining very precise servo performance. The unique and ultimate performance of the data acquisition module is essentially needed for suitability with the Chula2 manipulator system. We had to custom-design and build this data acquisition module to extremely appropriate for the Chula2 and to be excessive to support system enhancement that may be occurred in the future. According to the past experience with the Chula1 manipulator, we emphasized to avoid, as much as possible, treatment about analog signals. Digital techniques were preferred in any parts of the data acquisition unit. Since, digital signal is much immune to measurement noise than analog one. The application of optical encoder to measure both position and velocity reflects this point of view. Optical encoder is directly applicable to position measurement which is corresponding to the number of digital pulses generated from the encoder. Hence the frequency of that pulse train implies rotational speed of the encoder shaft. Unlike other systems that speed measurement from encoder signal is still to make use of analog measurement coming from application of the frequency-to-voltage converter which tends to be quite noisy, instead ,we used very accurate computer-controlled digital frequency counter to measure speed of rotation from encoder signal. In explanation of the unit, we will describes its function and performance according to all equipments we built.

Servo Data Processor (SDP)

This computerized digital circuits contains all necessary function for processing digital information from the encoders. The basic functional modules are long distance line receivers, decoders, position collectors or counters and frequency measurement circuits all controlled by a Z-80 single board computer. The unit features 6 encoder input channels and 3 counter displays of 10-digit resolution. The internal position counters can recognize up to 10 millions of encoder pulses redundant for the current joint resolution of the Chula2. For velocity measurement, the pulse-train period will be captured by the velocity capture logic circuits and the period time data will be processed into joint speed by the single board computer. Joint speed and position data retrieve will be serially transmitted to the SCS and the ECS independently to each other through the long-distance line driver circuits. This data transmission can contain position and speed data up to six joints with maximum cycle

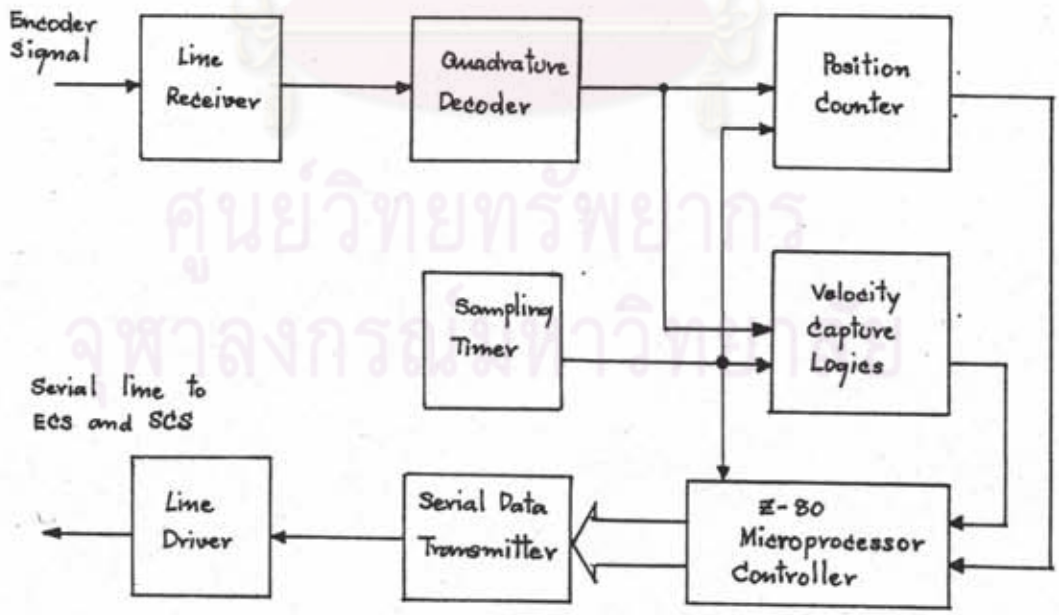

Figure 4.3: Functional block diagram of the SDP

period of less than 4 ms. This means that the SDP can simultaneously deliver servo data of six encoders allowing relevant servo controller to perform the maximum sampling rate of more than 250 Hz.

SDP-to-DMA Interface (SDI)

This is a PC/AT compatible interface custom-built for fast delivery of SDP data into the PC/AT compatible computer memory through the mechanism of Direct-Memory-Access (DMA). The operation of the interface has to be passively started from the programmed transient signal initially transmitted from the SDP. After starting up, the SDI will capture and recognize all serial data within its own memory and later frame it into 16-bit parallel data. At this moment after completely 16-bit data framing, the SDI will inject DMA request signal into the PC/AT system bus and common DMA cycle will be generated to transfer data into the computer memory. This

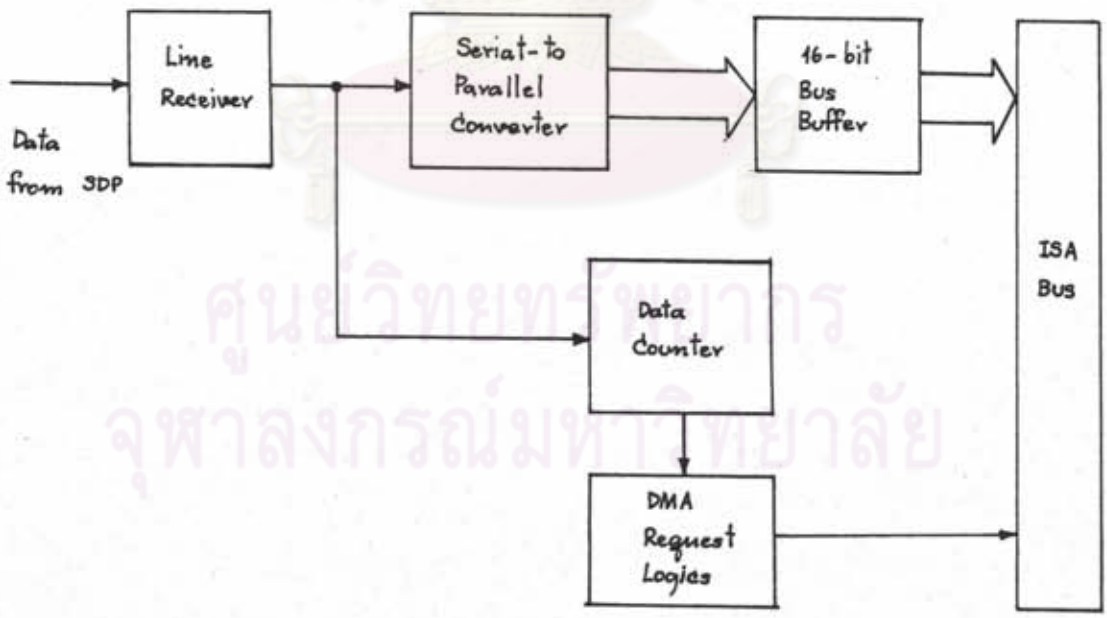

Figure 4.4: Functional block diagram of the SDI

operation will interfere the whole system bus cycle of the computer no more than 2% of the system bus bandwidth. There are two of this interfaces installed into the open bus of the SCS and the ECS for simultaneously receiving position and speed data gaining degree of parallelism to the computing system.

General I/O Interface (GIO)

The interface features analog and digital I/O for general control and data acquisition purpose. 24-bit of digital I/O was specifically designed for controlling the power supply unit and supporting parallel communication between the two PC/AT compatible microcomputers. Cooperation with the API card installed in the 80386 microcomputer, asynchronous parallel

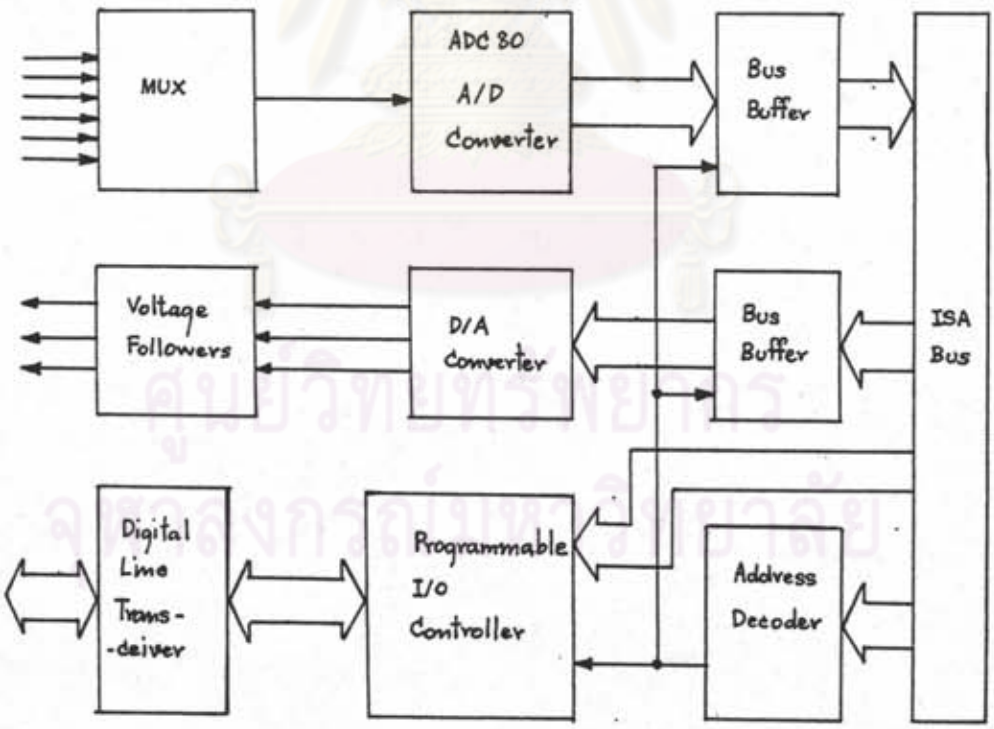

Figure 4.5: Functional block diagram of the GIO

communication between the two computer can be rapidly taken place. Installed with the GIO, the SCS can absolutely control all function of the three LA-5600 amplifiers. In addition, the GIO digital inputs are used to monitor current operating condition of the amplifiers. The analog part comprises an Analog-to-Digital (A/D) converter for analog signal measurement and Three Digital-to-Analog (D/A) converters for delivering analog control output. Both are used with the amplifiers. The A/D function is to sense the MCO signals to incorporate torque information into the control scheme. The D/A are exploited to inject voltage signal to command the amplifiers a amount of motor current needed for servoing through the VCS ports.

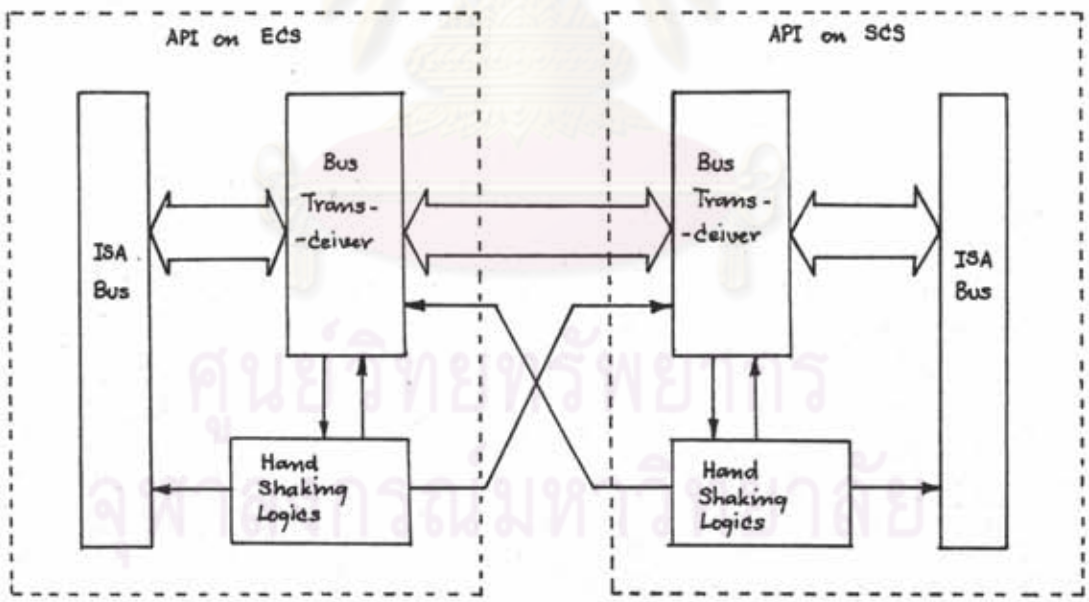

Figure 4.6: Functional block diagram of the APIs.

Asynchronous Parallel Interface (API)

The function of this customized interface is to offer bidirectional communication between the SCS and the ECS. The interface design is making use of the rapid PC/AT interrupt structure and IEEE standard bus driver to obtain fast and precise asynchronous data transfer. Its structure is composed from standard VLSI building blocks in a simple manner to achieve the function. The custom-built external bus has a frequency bandwidth of around 30 MHz which is approximate to a bandwidth of PC/AT open bus architecture. Hence, the design leaves the interrupt mechanism of the PC/AT the slowest portion of the transfer instead of the interface bus delay.

C. Power Supply Unit (PSU)

The unit comprises three sets of servo amplifiers for driving DC servo motors of the joints. The servo amplifier can be programmed to act velocity servo loop of a motor or to be as a current amplifier for exerting an exact amount of DC current, according to a torque command from the servo controller to a motor. The latter is our case that the cooperation of the current amplifier and a corresponding DC motor allows the dedicated servo controller to linearly command and exert an exact amount of torque to the manipulator mechanism.

Three Electro-craft model LA-5600 linear servo amplifiers were chosen to drive the three joint motors. They are capable of supplying 22 Amps peak current to motors for intermittent operation. The output current is electronically limited to provide protection for the amplifier and the servo motor. The LA-5600 amplifier has a peak current limit circuit which limits the maximum current available from the amplifier. The RMS current limit circuit is also provided as for limiting the length of time excessive current is applied to the motor. The basic operation of the amplifier can be occurred in the four quadrants of the torque-speed relation in addition to normal operation of the motor and the amplifier interconnection which is usually performed in the first and the third quadrant

torque and speed have different sign the amplifier is then fell into the dynamic braking mode. This is a special condition where the motor acts as a generator decelerating the attached load and its own rotor. During dynamic braking, the kinetic energy stored in moving parts of the motor-load interconnection will be turned to be electrical power in the form of direct current fed back into the amplifier. This electrical power will then be dissipated at the output stage of the amplifier in the form of heat.

The amplifier set has two analog inputs; VCS and AUX, that will be summed together to get a reference command to the inside operational amplifier acing as a summing junction in the feedback loop. In our case, we only use the VCS input as a current reference input to the current amplifier. The amplifier also generates two analog output signals; MVO and MCO, which may be used for servo feedback purpose. The Motor Velocity Output (MVO) signal is an analog voltage signal which is proportional to the actual instantaneous motor speed. The signal is obtained from the buffered tachometer voltage input to the amplifier. The Motor Current Output (MCO) which comes from the internal current sensing circuit is an analog voltage signal proportionally indicating the amount of the instantaneous motor current consumption and consequently also indicative of motor generated torque at that moment. When operating in the current amplifier mode, we will disconnect the tachometer feedback signal leaving only the MCO to be sensed as motor torque feedback signal incorporating with control scheme implemented.

For the purpose of amplifier control, the amplifier offers internal clamp circuits used to limit operating range or restrict the function of itself. In the Chula2 system, we built an interface circuit between the SCS and the amplifier clamps. All function of the amplifiers are completely controller by the microcomputer including safety mechanism that the microcomputer will automatically cut off the amplifier when the arm reaches clockwise or counter-clockwise limits. Furthermore, the interface will allow the external clamping circuit to exert clamp inhibit signal in parallel to the microcomputer command. This external clamping circuits which receive joint inhibit

parallel to the microcomputer command. This external clamping circuits which receive joint inhibit signal from the infrared sensors installed at the manipulator joints will act as the second safety mechanism always working, though facing with computer failure.

4.2 Experimental Evaluation

So far, we have discussed the method of deriving a mathematical model of a manipulator and established physical insights about particular characteristics of manipulator dynamics to realize inherent physical complication of a manipulator as a highly-nonlinear controlled plant. An indirect adaptive control scheme for a manipulator exploiting the certainty equivalence approach proposed in (6) is chosen to be implemented as our manipulator control case study. Relevant theoretical backup was laid down to support for the scheme's practical validity. Detailed explanation of designs and /construction of the Chula2 manipulator was presented to introduce mechanical structures and its associated control equipments for that the manipulator system will base our experimental evaluation on the practical applicability of the adaptive scheme. We now already have adequate background to go on into actual hardware experimental study. A set of control experiments is established in such a way that will reflect promising potential of the adaptive control performance under real operating environment, that should exhibit significant difference among the results inferred from theoretical study, obtained from computer simulation, and actual hardware operation. As the Proportional-Derivative control still acceptably proved itself to be effective in controlling an indirect-drive, low speed robot as the Chula2 is, the experiments with PD implementation will also be carried out under the same operating condition to offer comparable results to compare to the adaptive performance. According to our theoretical consideration, we know that the strong advantage of the indirect adaptive control lies upon the ability of the on-line estimator to capture the effects of uncertainty in parameters and unmodeled dynamics at once in the resulting estimated model. Since our manipulator adopts high ratio speed reducers in order to amplify the amount of joint actuating torques, the influence of that uncertainties is then greatly scaled down by a factor of the square of the speed

reduction ratio. Hence, under normal operating conditions, general tracking operation of the manipulator seems to be too smooth for the adaptive control to display its control capability. As a result, we need to exaggerate effects of dynamic uncertainties in the experiments to deliver " worse" environment where the conventional fixed-gain controller is expected to be taken into the limit of its robustizability, while the adaptive control is predicted to significantly outperform the PD. In this way, adaptive performance should be exposed to us and the objective of the scheme's justification will be satisfied.

4.2.1 Dynamics of the Chula2 Manipulator

According to the Denavit-Hartenberg notation described in Chapter 2, the way we assign the coordinate systems into the Chula2 linkage is depicted in Figure 4.7.

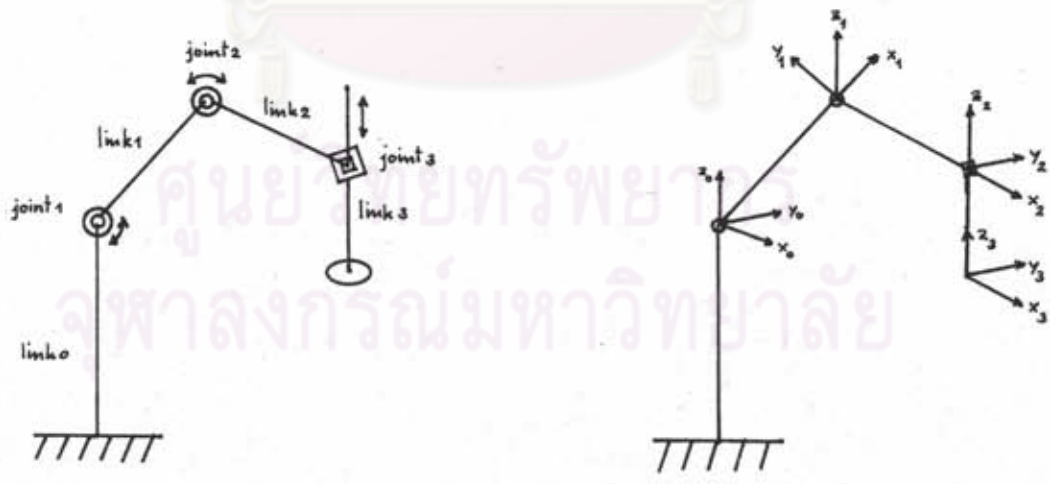

Figure 4.7 : Affixing coordinate frames

We note that joint n is defined to be a joint connecting link n-1 and link n. The link numbering begins at link 0 that is considered to be dynamically fixed with respect to the earth ground and will preserve as the inertial frame of reference of the whole dynamic discussion in the consequence. The coordinate frame assignment is done in the way that the coordinate frame n will be of link n, i.e., it is rigidly attached to link n, and its z-axis is coincident with joint n+1 axis. As a consequence, we see that we can describe the current position and orientation of a body of link n implicitly by the current description of the coordinate frame n in terms of the coordinate frame n-1. Therefore, the angle that the frame 1 rotates around the z-axis of the frame 0 amounts to the joint coordinate θ_1 and so on for θ_2. For joint 3 that performs translation, the joint coordinate d amounts to vertical distance made by frame 3 measured with respect to the z-axis of frame 2. The following table summarized Chula2 link parameters and joint variables.

link	*variable*	$a(m.)$	α	$d(m.)$	θ
1	θ_1	0.7	0.0^o	0.0	θ_1
2	θ_2	0.4	0.0^o	0.0	θ_2
3	d_3	0.0	0.0^o	d_3	0.0^o

Table 4.1 : Link parameters and joint variables of the Chula2 manipulator.

Recall the definition of the A matrix describing geometrical relation between consecutive linkages, we substitute the above values of link parameters into the matrix, we immediately obtain the following kinematic descriptions, for brevity of term presentation, c_i, s_i, c_{ij} and s_{ij} are used to denote $\cos\theta_i, \sin\theta_i, \cos(\theta_i+\theta_j)$ and $\sin(\theta_i+\theta_j)$ respectively,

$$\mathbf{A}_1 = \begin{bmatrix} c_1 & -s_1 & 0 & a_1c_1 \\ s_1 & c_1 & 0 & a_1s_1 \\ 0 & 0 & 1 & 0 \\ 0 & 0 & 0 & 1 \end{bmatrix} \qquad (4.1)$$

$$\mathbf{A}_2 = \begin{bmatrix} c_2 & -s_2 & 0 & a_2c_2 \\ s_2 & c_2 & 0 & a_2s_2 \\ 0 & 0 & 1 & 0 \\ 0 & 0 & 0 & 1 \end{bmatrix} \tag{4.2}$$

$$\mathbf{A}_3 = \begin{bmatrix} 1 & 0 & 0 & 0 \\ 0 & 1 & 0 & 0 \\ 0 & 0 & 1 & d_3 \\ 0 & 0 & 0 & 1 \end{bmatrix} \tag{4.3}$$

With respect to the base frame, the kinematic equations are as follows.

$$\mathbf{T}_1 = \mathbf{A}_1, \tag{4.4}$$

$$\mathbf{T}_2 = \mathbf{A}_1\mathbf{A}_2 = \begin{bmatrix} c_{12} & -s_{12} & 0 & a_2c_{12} + a_1c_1 \\ s_{12} & c_{12} & 0 & a_2s_{12} + a_1s_1 \\ 0 & 0 & 1 & 0 \\ 0 & 0 & 0 & 1 \end{bmatrix}, \tag{4.5}$$

$$\mathbf{T}_3 = \mathbf{A}_1\mathbf{A}_2\mathbf{A}_3 = \begin{bmatrix} c_{12} & -s_{12} & 0 & a_2c_{12} + a_1c_1 \\ s_{12} & c_{12} & 0 & a_2s_{12} + a_1s_1 \\ 0 & 0 & 1 & d_3 \\ 0 & 0 & 0 & 1 \end{bmatrix}. \tag{4.6}$$

Using the manipulator kinetic energy expression (2.22), we then have the closed form of the kinetic energy of the Chula2,

$$K = (A + B\cos\theta_2 + C\sin\theta_2)\dot{\theta}_1^2 + (D + B\cos\theta_2 + C\sin\theta_2)\dot{\theta}_1\dot{\theta}_2 + \frac{1}{2}D\dot{\theta}_2^2$$

$$+\frac{1}{2}m_3\dot{d}_3^2 \tag{4.7}$$

where

$$A=\frac{1}{2}\Big[I_{1zz}+I_{2zz}+I_{3zz}+\left(a_1^2+2a_1\bar{x}_1\right)m_1+\left(a_1^2+a_2^2+2a_2\bar{x}_2\right)m_2$$

$$+\left(a_1^2+a_2^2+2a_2\bar{x}_3\right)m_3\Big]$$

$$B=a_1\Big[\left(a_2+\bar{x}_2\right)m_2+\left(a_2+\bar{x}_3\right)m_3\Big]$$

$$C=-a_1\left(\bar{y}_2m_2+\bar{y}_3m_3\right)$$

$$D=\frac{1}{2}\Big[I_{2zz}+I_{3zz}+\left(a_2^2+2a_2\bar{x}_2\right)m_2+\left(a_2^2+2a_2\bar{x}_3\right)m_3\Big]$$

While the amount of its potential energy can be written as

$$P=-g\Big[m_1\bar{z}_1+m_2\bar{z}_2+m_3\left(\bar{z}_3+d_3\right)\Big] \tag{4.8}$$

Finally, according to (2.39), we can then write the completed equations of motion as follows,

$$\tau_1=2\big(A+B\cos\theta_2+C\sin\theta_2\big)\ddot{\theta}_1+\left(D+B\cos\theta_2+C\cos\theta_2\right)\ddot{\theta}_2$$

$$+\left(C\cos\theta_2-b\sin\theta_2\right)\left(2\dot{\theta}_1\dot{\theta}_2+\dot{\theta}_2^2\right) \tag{4.9}$$

$$\tau_2=\left(D+B\cos\theta_2+C\sin\theta_2\right)\ddot{\theta}_1+D\ddot{\theta}_2+\left(B\sin\theta_2-C\cos\theta_2\right)\dot{\theta}_1^2 \tag{4.10}$$

$$f_3=m_3\ddot{d}_3-m_3g \tag{4.11}$$

where τ_1 and τ_2 are driving torques of joint 1 and 2 respective;y, delivered from power transmission systems consisting of joint actuators and speed reducers to manipulator linkage. f_3 represents linear force that drive link3 to translate in vertical direction.

From the above, we can observe some difficulty emerged in the Chula2 equations of motion. Despite the SCARA configuration of the Chula2 makes the kinematic terms so simple, we still face with a large dynamic structure even the expression are formulated for only three joints.

4.2.2 Experimental Implementation

Figure 4.4 shows the way that we implement the adaptive control presented in Section 3.1. on The Chula2 controller system. As described in Section 4.2., two industry standard microcomputers are used to serve as two concurrent computing modules for sufficiently delivering computational power to support Chula2 operation. The SCS is implemented to perform basic servo calculation upon receiving joint motion information, to control all hardware of the Chula2 controller. We shall detail the configuration and cooperation of the SCS, the ECS, and connected hardware. As shown in Figure 4.3, on the ISA bus of the SCS microcomputer we have installed three customized interface cards, namely, the SCI, API, and GIO. In operation of the implemented servo loop, the SDP will compute and collect encoder data continuously within its counter memory. The current available data will be transformed by CPU of the SDP into digital words indicating joint position and velocity values, and then will be serially transmitted to both the SCS and ECS. the SDI modules on that two computers are responsible for interfacing this transmitted information with particular memory location whose addresses are preset by main software of the computers. Thereby, with this mechanism, the joint moving data can be flown into memory of the two computers without processing attention of the main programs. The rate of this transmission can be achieved at about 650 cycles per second for three joint data acquisition. To calculate servo errors and control efforts, the

will look at that particular memory location for current joint data and perform the calculation, and thereafter the results will be sent to the D/A converter unit on the GIO. In this way, the basic servo control can be completed within the SCS itself allowing the ECS to utilize its full computing capability on the identification algorithms. The achieved PD servo rate delivered from the SCS stand-alone implementation is more than 400 Hz fast enough to support control implementation in a continuous-time fashion.

We had constructed a mechanism of correspondence facilities to serve the need of rapid data transfer between the algorithms implemented on the two microcomputers. The correspondence

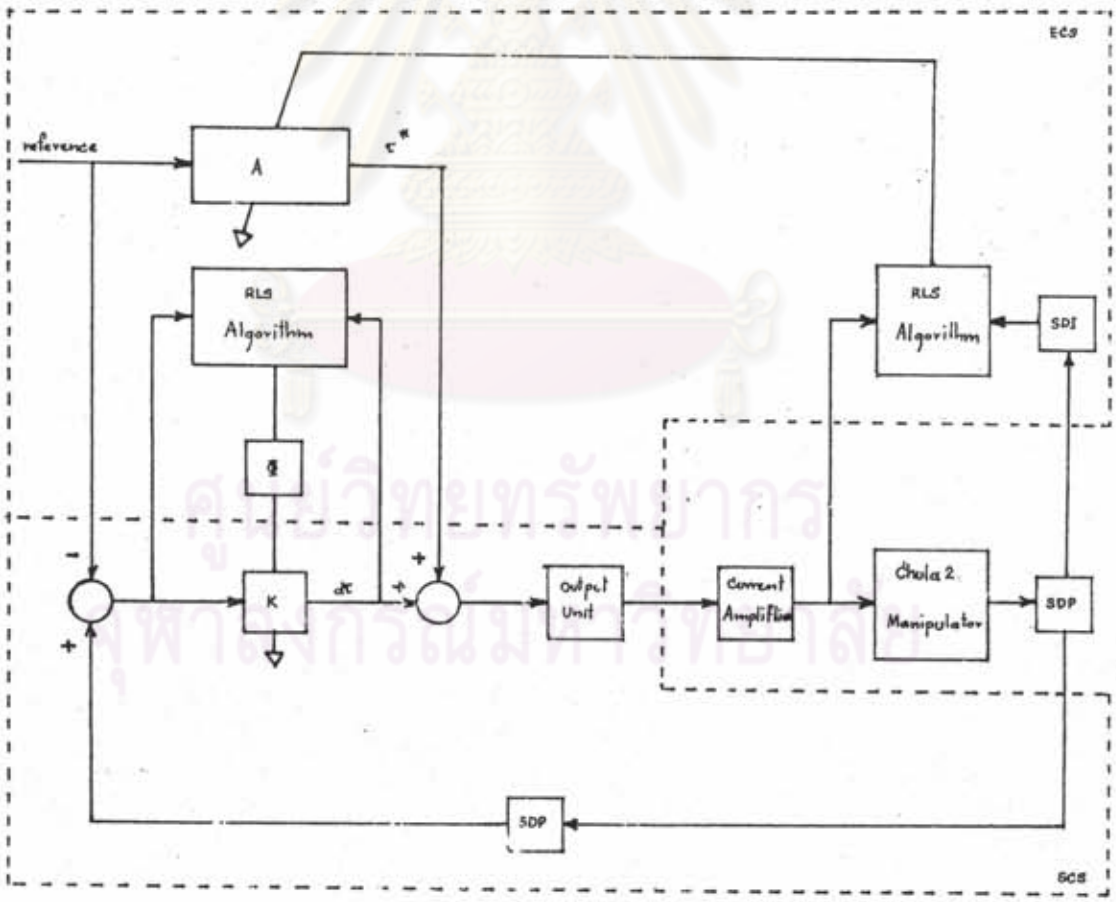

Figure 4.8: Implementation of the adaptive control on the Chula2 manipulator system

software module on the SCS takes control of all data transfer operations. Its transfer mechanism is designed to be versatile, and can be reprogrammed to in a way that will most suit for the implemented scheme. The correspondence on the ECS is a passive functional block whose response depends on commands from its counter part on the SCS. All software functions are timed by a sampling control timer of the SCS, its operation stems from a programmable digital hardware timer built in the GIO card, hence can provide very precise timing for each software module through the microcomputer interrupt mechanism.

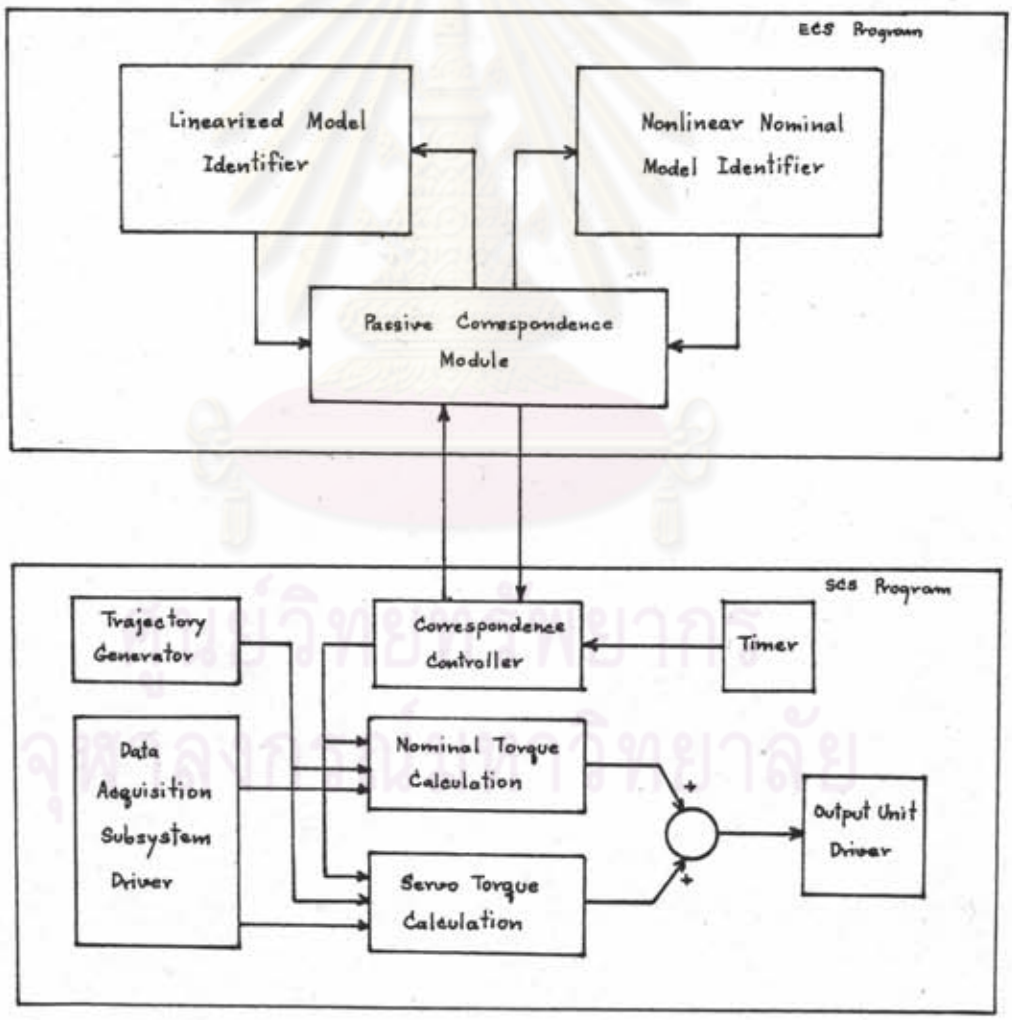

Figure 4.9: Software implementation.

Software design is based on the certainty equivalence scheme in Section 3.2. The strategy of software implementation is that all adaptive algorithms are separated from the basic servo computation and implemented in the ECS computer. Two levels of system identifications constitute the whole adaptive algorithms. one is the identification of the linearized perturbed dynamics characterized by the matrix incorporated within that is used to compute the LQ optimal gains. Another performs identification of the nominal system described by the matrix A and is installed inside the module that computes the nominal torques. Hence, the results that are to be sent back the SCS are that of the nominal torques and the optimal gains K. It should be, however, noted that the computation of the two values occurs at different rate. According to (6), the nominal torque was computed at every trajectory point, while the computation of K was taken place twice rate of that, the same as the rate of control loop sampling. Our tack will follow the method, but with little modification.

The implementation also recognizes precautions from theoretical development. As they had been detailed in Section 3.3, the validity of a certainty equivalence control law to be applicable in practical situation relies heavily on an important assumption that the model identification or the equation of parameter update must be performed slowly with respect to the actual closed loop dynamics. The implementation rate of K relative to that of the servo reflects this point of view. Since, the presence of the nominal torque is to address an instantaneous operating point along trajectory for the linearized perturbed model to be validly expanded, the rate of the nominal torque calculation should be slower that the rate of computing Φ and K and should be the same as the rate of trajectory point update.

All algorithms were written in C language exploiting single precision floating point arithmetic running on the Intel processors. Their machine codes was obtained under Turbo C compilation. The reason behind the selection of the arithmetic relies upon the necessity to compromise numerical performance on the basis of having small round-off error, while retaining

high speed calculation in order for possessing sufficient sampling rate. As a result, we obtain the servo running at a rate of 200 Hz, the optimal gain K is updated at a rate of 40 Hz, and the nominal torque is computed at the same rate as the trajectory update that is at 20 Hz twice times that of K as implemented in (6).

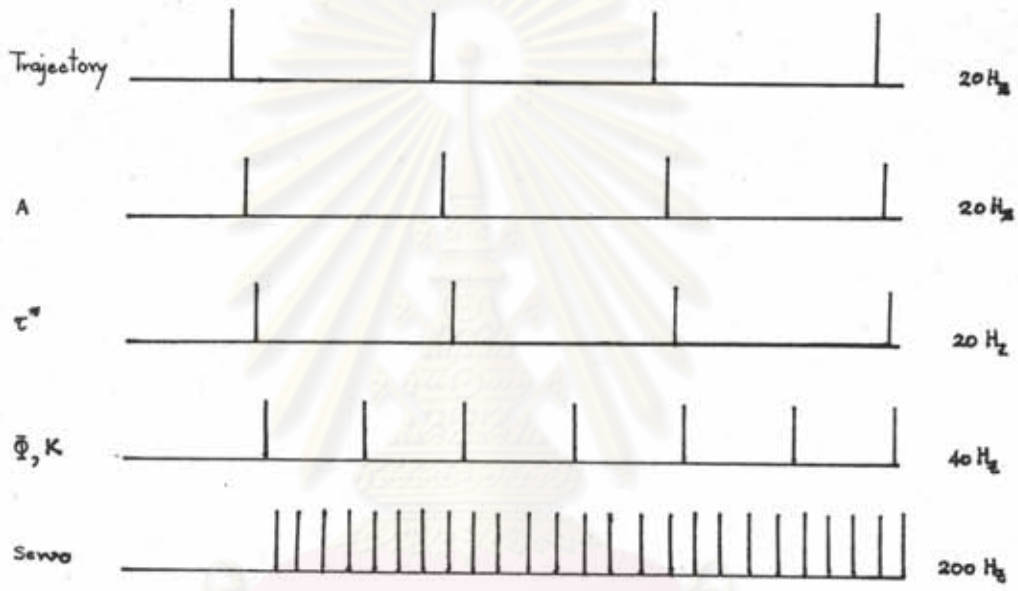

Figure 4.10: Timing of algorithm calculation

4.2.3 Experimental Results and Discussions

Three sets of experiments were established to demonstrate stability and robustizability of the indirect adoptive control via path tracking performance characteristics. To make the results comparative with those of conventional path tracking controllers, the PD controller was also implemented to perform the same sets of experiments with the same operating environment. Excluding the need to examine the basic tracking performance of the controllers, the experiments were conducted to reflect two aspects of advanced control performance, in which the certainty

equivalence control law is expected to offer significant advantages over the conventional fixed-gain controller according to our previous theoretical development. The first is to show capability of the adaptive control to compensate small uncertainty in parameters during control operation. This small effect can be captured by virtue of the identification of the linearized perturbed dynamic model and corresponding compensation comes from the serve with the adaptive optimal gains. This aspect was tested in the first two sets of the experiments. The second aspect is inspired from advanced feature of the identification of the nominal dynamics. The actuating torques that are to be sent to the identifier module should reflect an actual amount of the needed torque at that instant. Hence, the effects of parameter uncertainty and unmodeled dynamics including external loading should be recognized at once in the quantity of the nominal torque. The third set of experiments aims at examining the controller under unmodeled dynamics by introducing large load disturbance to the manipulator while tracking the desired trajectory. All the experiments were done with the first two links of the manipulator. Inclusion of the third link adds no benefit to our justification on the adaptive control. Since, the third link dynamics are naturally decoupled from those of the first two links. This stems from the SCARA configuration of the manipulator as can be observed from the equations of motion in the previous section. Apart from this reason, the inclusion of link 3 will make up considerable computational burden to the microcomputer controllers as the associated matrix manipulation will diverge.

The desired trajectory used in all the experiments were the same, obtained from commanding the first two links of the robot to follow trapezoidal velocity path between Home position, $\mathbf{q}$ = [0.0, 0.0] rad., and the destination, $\mathbf{q}$ = [3.0, 2.0] rad., with various averaged tracking speed. Off-line trajectory calculation was used, and the results were already stored in the computer's memory before tracking operation began. The third experiment set was designed to be carried out at rather tracking, in which the PD performance is expected to degrade due to its fixed-gain feature that is unable to compensate for large velocity-dependent nonlinearity, and the condition was made more severe by adding 20 kg. load into the end of link 3 at $t = 1$ sec. This

aims to exaggerate dynamic effects in order to achieve reasonable justification from appropriate experimental results specifically originated from our manipulator which is an indirect-drive manipulator exploiting high ratio speed reducer, that all dynamic effects at the transmission system output side will be scaled down, when consider the effects at the actuators, by the square of the speed reduction ratio as mentioned before.

In experiments, the PD control was tuned to have its best performance under the condition of the first experiment set, i.e., the PD gains were selected to make the overall system nearly critically-damped when running trapezoidal velocity path at averaged speed 0.5 rad/sec. And these gains were fixed and used permanently with the other two conditions. The followings summarize their values.

$$K_{p_1} = 1{,}100 \text{ N.m./rad.}, \; K_{p_2} = 200 \text{ N.m./rad.}$$
$$K_{d_1} = 10 \text{ N.m.sec./rad.}, \; K_{d_2} = 50 \text{ N.m.sec./rad.}$$

The above values of the PD gains were approximated by performing a number of experimental trials. They just represent nearly best values at that condition, small changes in their values could not result noticeable changes in control response. However, their order of magnitude can increase more dynamic insights to us. With respect to the same critically-damped response which we infer the above values of the gains, it should be said that link 1 faces much more damping than link 2 , hence, the control is needed to add a few of K_{d_1} to the system, while a large value of K_{p_1} is needed to overcome large moment of inertia of link1. This reflects the fact, we have known before from its design, that joint 2 should be much more dexterous than joint 1 due to the use of very low inertia moving-coil motor as the actuator af joint 2. Rather large value of K_{d_2} should be interpreted that, by its own mechanical combination, the damping is rather too small to cause critically-damped response, thus, most of the damping required has to be acquired from the control.

For the indirect adaptive control, we reduced the number of the design parameters involved to a limited value in order to ease our experimental consideration. Referring to the one-step-ahead optimal regulator, the weighting matrices $\mathbf{Q}$ and $\mathbf{R}$ is presumed to be non-negative and positive definite respectively and are left for the designer to choose their specific values to penalize the performance index as desired. The choice of $\mathbf{Q}$ and $\mathbf{R}$ can affect stability of the regulator as can be evident from theoretical results. It should be realized that total value of the performance index is not important to the solution of the optimization, hence to the control properties of the resulting regulator. But in fact, it is, instead, the relative proportion between the servo error cost and the control effort cost comprised to be the index that can essentially affect the control. The larger control weighting with respect to the servo error weighting will yield a regulator that tends to stabilize the overall system with large servo error by a limited amount of the control effort. In converse, the larger error weighting will result in a good tracking accuracy regulator without concern of how much control energy will be dissipated. The latter can cause system instability in the final due to excessive exertion of the control effort.

Our selection was based upon the primary objective that is to obtain stable regulator performance. From asymptotic stability proof in Section 4.3, the third condition for the one-step-ahead LQ regulator to be asymptotically stable is that the first recursive matrix solution, $\mathbf{P}_1$, of the associated RDE must always be smaller than the initial condition, $\mathbf{P}_0$. The choice of the initial condition is arbitrary and can be specified via the selection of $\mathbf{Q}$. From theoretical point of view, there is no direct way yet to guarantee that condition. What we can do at best is to take to guarantee that the value will be large enough to be larger than any possible value that may occur, but this contradicts the aspect of practical implementation. The best way we could do under this circumstance is that we choose $\mathbf{Q}$ to be large and justify it with experimental trials, and then we can choose R to be small with respect to $\mathbf{Q}$. For simplicity, we choose the weighting matrices to be diagonal and all diagonal elements of each matrix have the some positive scalar values as can be expressed by the followings.

$$\mathbf{Q} = a\mathbf{I}, \quad a > 0,$$
$$\mathbf{R} = b\mathbf{I}, \quad b > 0.$$

The experimental trials were done under the condition of the first experimental set as in the case of find the PD gains. The trials began with fixing $b = 1$ and ended with $a = 10{,}000$ which seemed to deliver very good tracking at the condition. In conclusion, $a = 10{,}000$ and $b = 1$ were used throughout the experiments. The results of the three sets of experiments are illustrated in Figure 4.11 - 4.16.

Figure 4.11 displays tracking performance of the PD control at 0.5 rad/sec. averaged speed. At this rather low speed, the PD shows smoothness of trajectory tracking with the servo error being within 0.05 rad. for joint 1 and 0.06 rad. for joint 2. We observe that the final error at the destination with zero velocity are 0.015 rad. and 0.024 rad. for joint 1 and 2 respectively. These results represent nearly perfect tracking caused from tuning the controller to obtain its best performance. The fundamental source of this steady-state error mainly came from the presence of the deadzone nonlinearity in electromechanical composition of the manipulator joints. A set of a D/A converter and an amplifier posses a small range of inactive digital command that will not be able to activate the amplifier to deliver electrical power to a joint motor. Furthermore, the structure of joint mechanical composition makes up a certain amount of static, Coulomb, and viscous friction, that the joint motor has to overcome before being able to move the mechanism. Therefore, in order to command the manipulator joints to move, digital commands referring to amounts of actuating torques must be larger than a certain value that represent the size of the deadzone.
However, the problem may be solved directly by increasing the proportional gains so that small error can be scaled up by the gains to represent a larger amount of actuating torques, hence, forces the control system to further regulate small servo error. However, this means may violate smoothness

of error regulation characteristics of the control system as it could introduce oscillatory effect to the system.

A large amount of measurement noise is observed in measurement of joint velocity. Since, it was at first time that this manipulator system was officially tested and operated. Hence, there was no attempt, at that time, to correct the measurement. It can be observed that there was high frequency noise distributed throughout the velocity tracking history. The situation was more severe in velocity measurement of joint 2. This noise characteristics expose a fact to us that despite we made use of digital techniques throughout the design of the velocity acquisition system to avoid analog noise problem associated with tachometer feedback, we still face with considerable level of velocity noise as in analog case. Nevertheless, in tracking quality point of view, fluctuation in measured velocity did not disturb path regulation very much due to small derivative gain used.

The results on the indirect adaptive control are depicted in Figure 4.6 with no load at averaged tracking speed 0.5 rad/sec. As we can infer from theoretical development, the unloaded system, controlled using the nominal torque computed from the recursive least square identification, along with the optimal control of the estimated linearized perturbed model, tracks the desired trajectory. Furthermore, the results show better tracking error relative to the PD performance. For joint 1, the accumulated error along trajectory is reduced approximately by a factor of 2, and the maximum error decreases to 0.03 rad. While in joint 2, the system exhibited the same level of the maximum error, but its accumulated error also decreased. In addition, it is observed that the adaptive system tracks the desired trajectory with less smoothness than that of the PD. There exists fluctuation distributed over the error regulation characteristics. This causes from the operation of the nominal torque as can be observed in the output, nominal torques results. As we have discussed before, identification process is much sensitive to measurement noise, the fluctuation in value of the nominal torque and, as a consequence, of the tracking error should reflect this point of view.

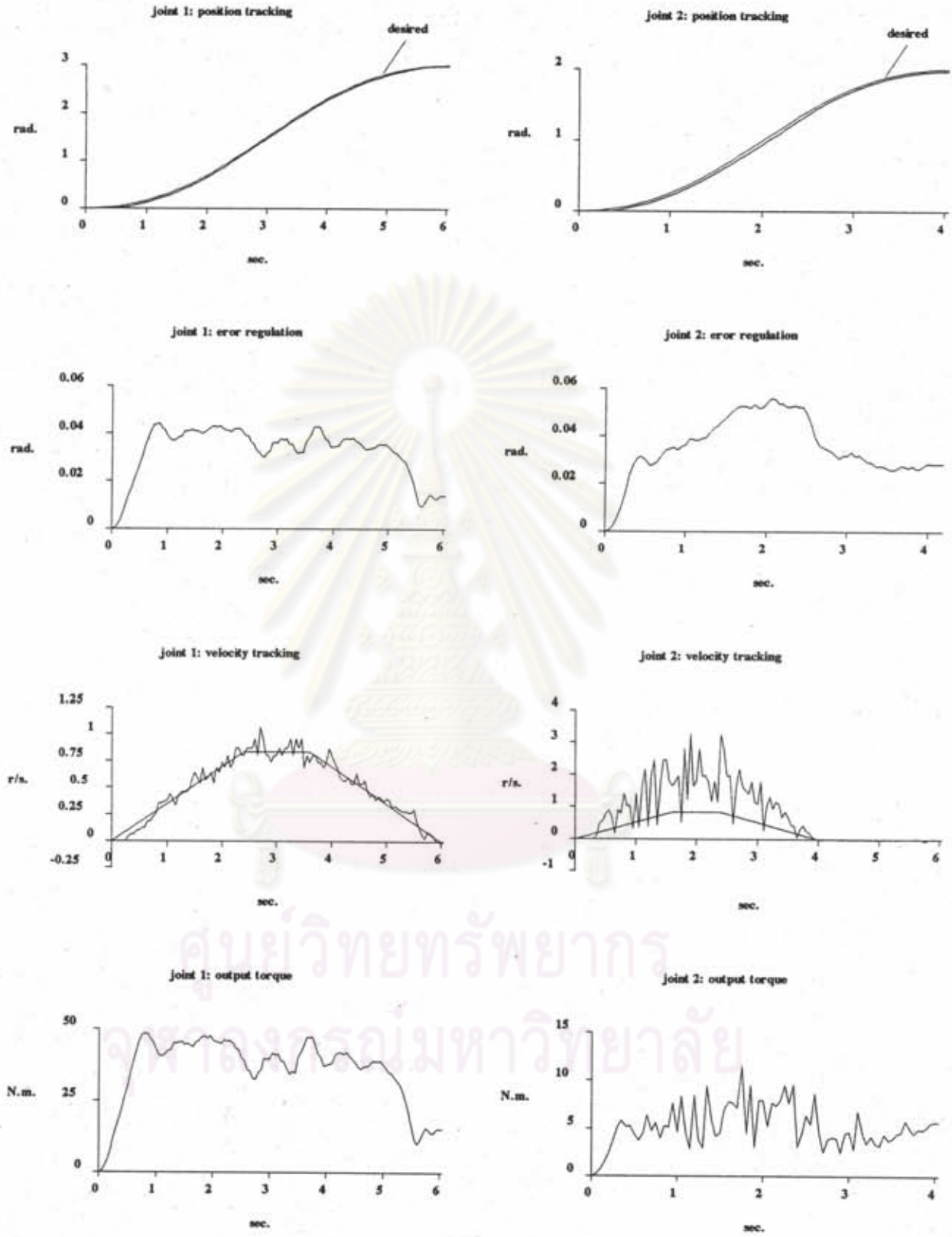

Figure 4.11: PD control with no load, averaged speed 0.5 rad/sec.

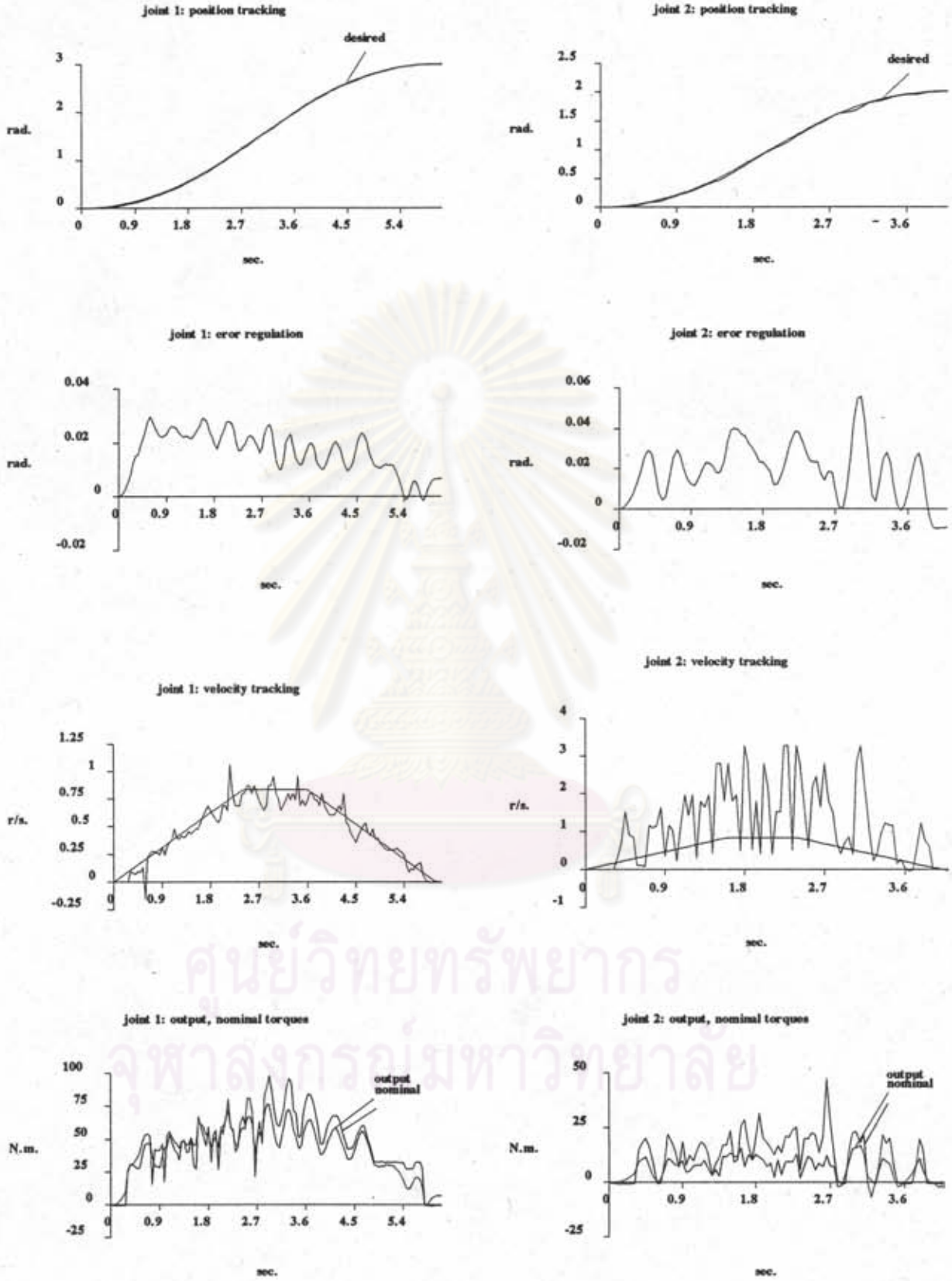

Figure 4.12: Adaptive control with no load, averaged speed 0.5 rad/sec.

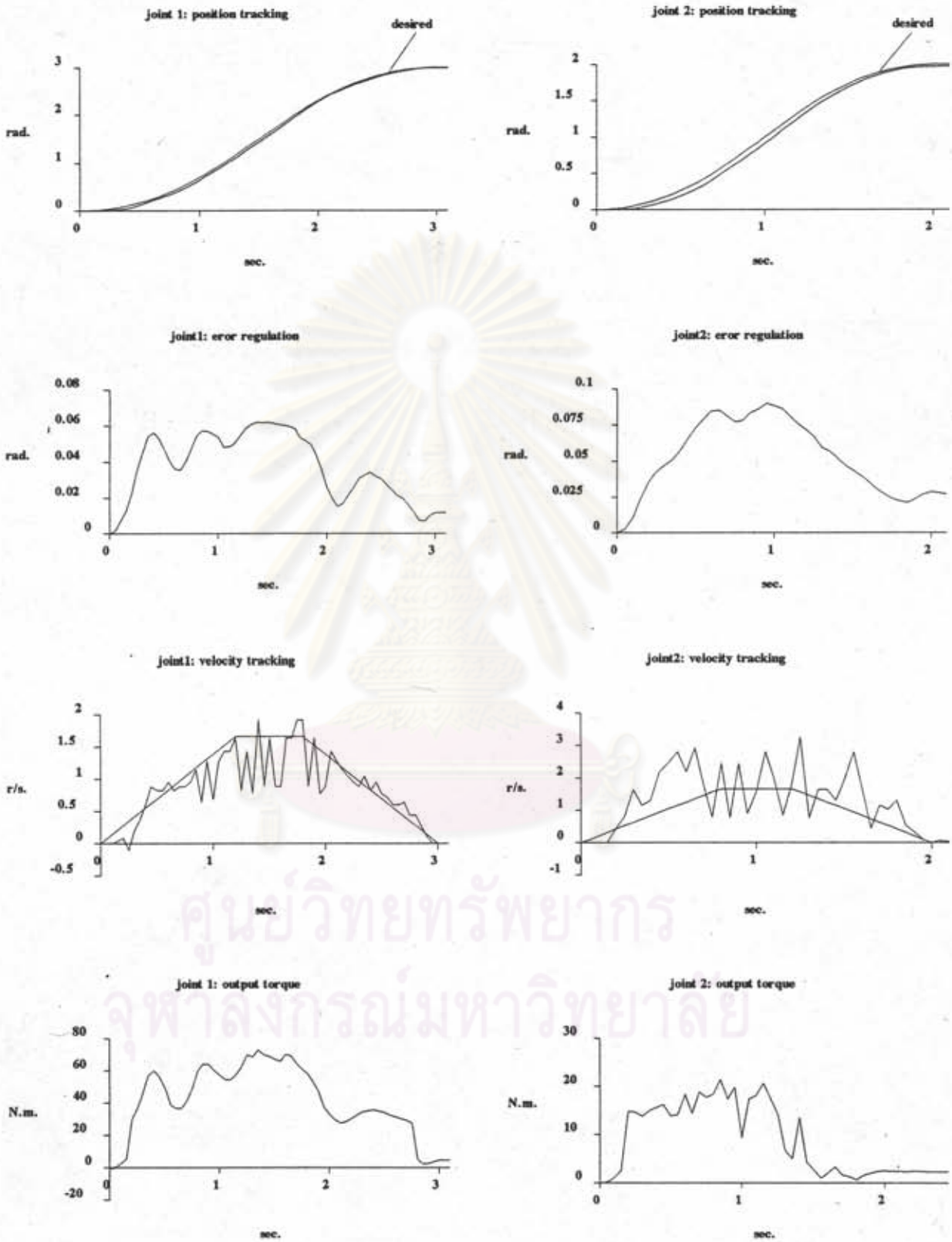

Figure 4.13: PD control with no load, averaged speed 1.0 rad/sec.

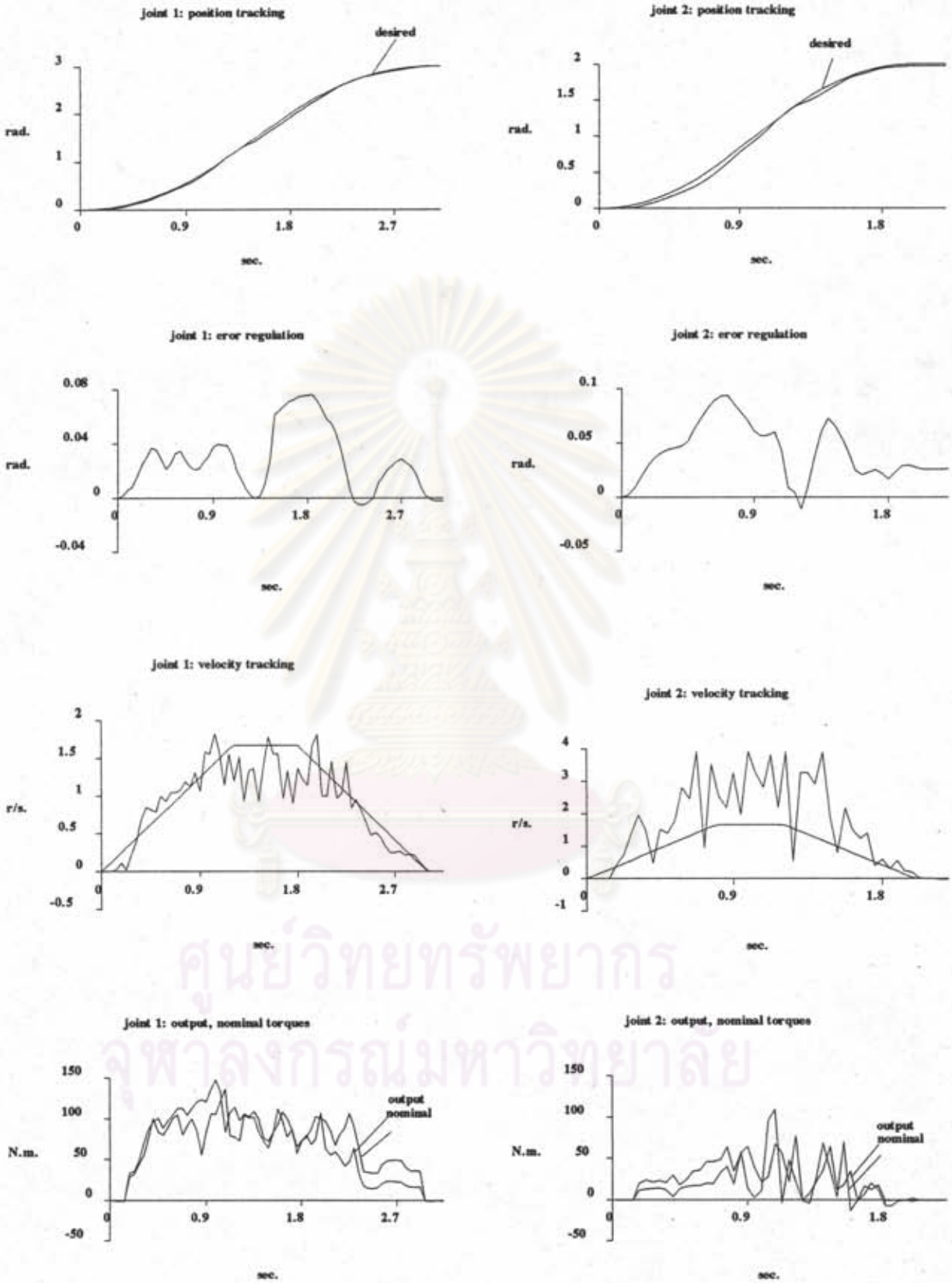

Figure 4.14: Adaptive control with no load, averaged speed 1.0 rad/sec.

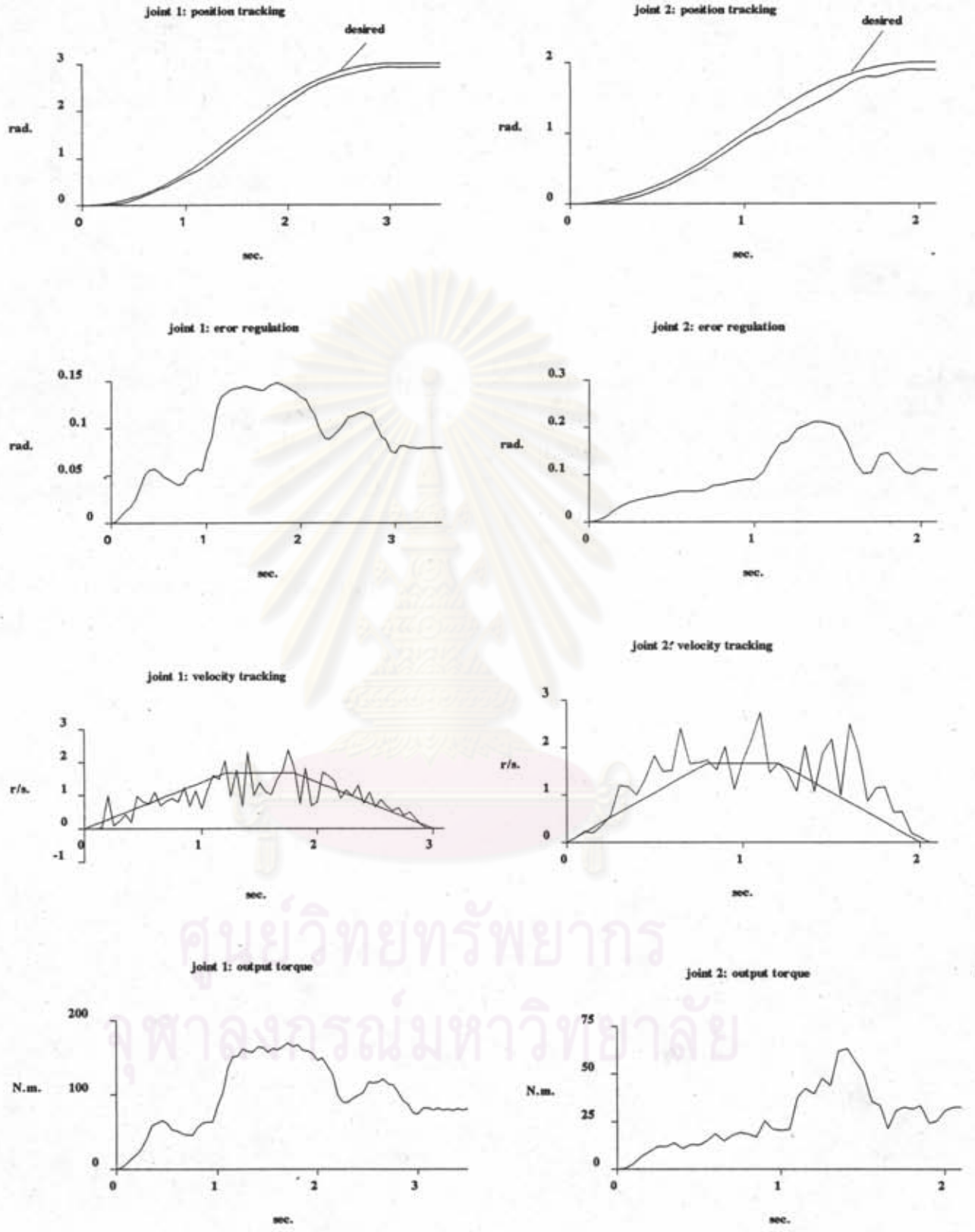

Figure 4.15: PD control with large load, averaged speed 1.0 rad/sec.

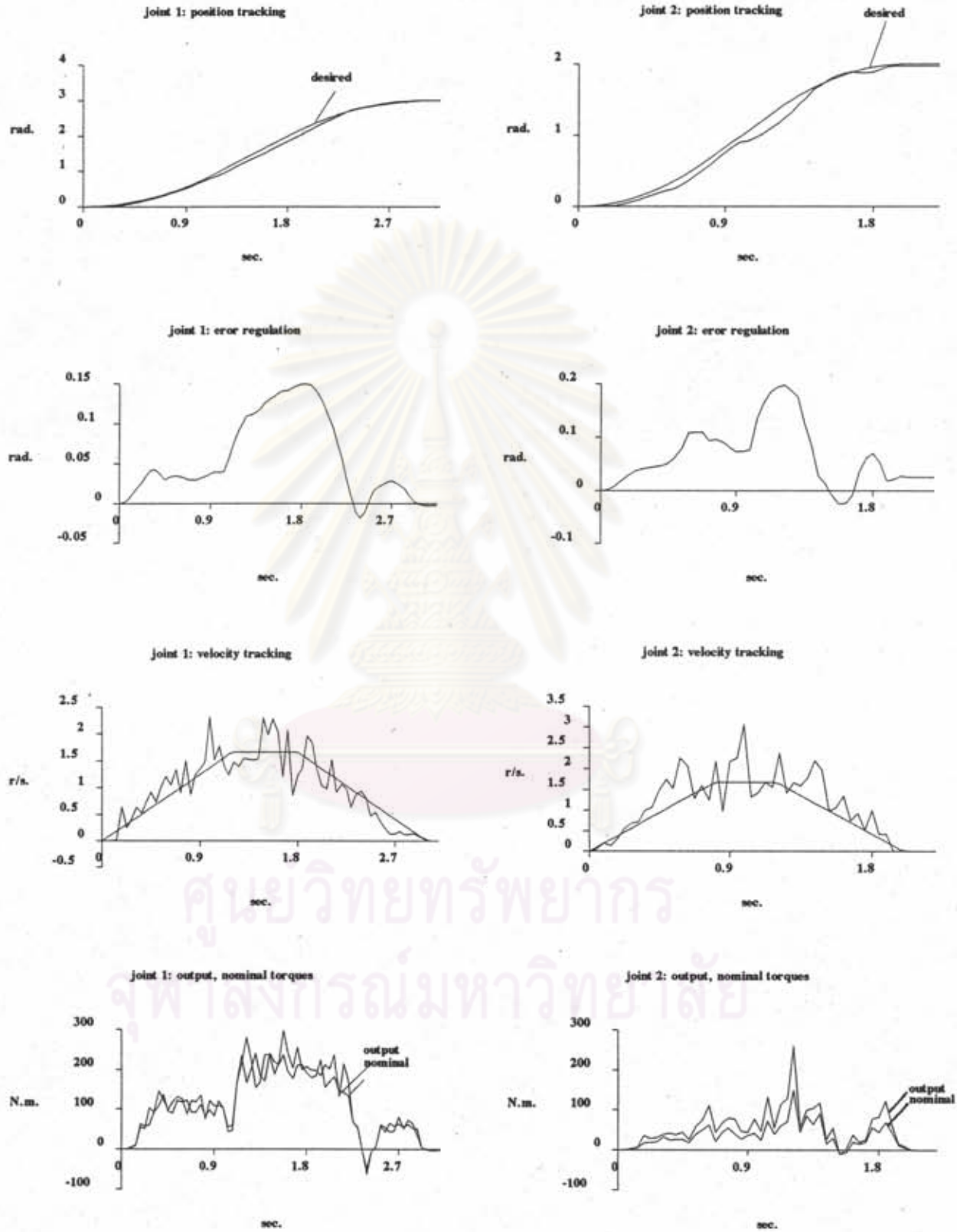

Figure 4.16: Adaptive control with large load, averaged speed 1.0 rad/sec.

As tracking speed is increased, it is apparent that the performance of the PD degrades. Since, the fixed-gain characteristics may be thought of as being equivalent to fixed performance at a selected condition, the critically-damped gains are no longer properly work. The PD gains that yield optimum performance at 0.5 rad/sec. seem to offer too stow response for a new, and faster trajectory. In the case of the adaptive control, We see a satisfactory advantage that speed of tracking response was automatically adjusted by adaptation to suitably track the new trajectory. The calculation of the nominal torque incorporates a next reference point from the desired trajectory so that the future effect of the trajectory is realized within the nominal torque value representing one-step expectation of the adaptive controller to address more proper actuating torque for trajectory tracking. The optimal regulator also serves this need, but in a faster time scale to handle higher frequency closed loop dynamics through the adaptation of the servo gains.

It may be concluded that under the adaptive control, the tracking error is generally better than that of the PD, while smoothness of error regulation is apparently poorer. In the sense of robustness, therefore, it can be said that the indirect adaptive control delivers no benefit to the conventional fixed-gain controller due to its high measurement noise sensitivity.

The second set of experiments was repeated with instantaneously increasing of the mass of the third link about 25% after t = 1 sec. The results are shown in Figure 4.13 and 4.14. If can be observed that as a result of this loading disturbance, joint 1 and 2 move away from the commanded trajectory and a large final error occurs. In joint 1, a final error was increased to be 0.075 rad., while in joint 2, the error is 0.13 rad.. The adaptive control results show a significant improvement over the PD control. After the mass of link 3 was perturbed at t = 1 sec., the adaptive control was still able to regulate the system to track the prescribed position. The error regulation results show the same level of the final error as occurred in the unloaded system. It should be noted that the effect of loading reflects in the identification of the nominal system dynamics and affects the nominal torque value as can be seen in the output, nominal torque results. Hence, after the loading effect

perturbed away the nominal operating point along the nominal trajectory, the identifier of the nominal dynamics realized this within the new identified model and the resulting nominal torque calculated using this model compensated for this effect readdressing a more proper operating point to make the linearization of the perturbed dynamics still further valid and the optimal regulator resulted from this perturbed model was still able to stabilize the system., and thus, the control system continued to track the desired trajectory after the transients from the loading perturbation had died out.

The experimental results has confirmed us that the applicability of the indirect adaptive control of a manipulator using the certainty equivalence principle incorporated with feed forward compensation from nonlinear identified model is available. Comparison with the PD in tracking performance., the adaptive control shows its advantages over the PD in three aspects. First, in all operating condition it delivers better tracking accuracy in terms of both the accumulated error along trajectory and the final error at the end position of a trajectory. Second, the tracking response characteristics of the adaptive control update continuously with current operating circumstance. Third, the adaptive control offers a significant improvement in dealing with unstructured uncertainties and in retaining stabilizability of the whole system in the face of undetectable external disturbance such as the insertion of mass perturbation in the third set of experiments. However, regulation characteristics of the adaptive control possesses more fluctuation than the PD, this can be interpreted that the PD has lower sensitivity to measurement noise than the adaptive. Therefore, in this sense, it can be said that the PD is more robust than the adaptive.

Despite we have theoretical results to support our experimental evaluation . The asymptotic stability proof of the one-step-ahead optimal regulator is just based upon the nominal plant model. The robustness results insist us that the stabilizing regulator designed on the basis of the nominal plant model will also stabilize the real plant that stays in the neighborhood of the model, provided that the difference between the real plant and the model is sufficiently small. But in spite of much of

our attempt spent to elaborate explicit size of this difference, there is no guarantee yet to confirm us how much the model we select to base the regulator design is far away from the real plant, because the real plant represents a thing that we never know its details exactly. To bridge this plant/model mismatch gap, model identification technique is introduced. The theoretical development further states that for a regulator design utilizing LQ methodology and for a plant model obtained from RLS identification, both incorporated within the same closed loop control system, the resulting difference between the real plant and the identified model will be guaranteed to be small enough to be within the robust region so that LQ regulator designed, based upon this identified model, will also stabilize the real plant, if restricted and smoothness conditions on the amount of unmodeled dynamics are satisfied. This pleasing result meets with our need to apply the certainty equivalence control law in practical system, but still relies upon many idealized conditions. Hence, control error and all of imperfection appeared in the experimental results stem from these sources of idealization in an attempt to apply theoretical results with the actual hardware system.